THE
PHYSICAL REVIEW
A journal of experimental and theoretical physics established by E. L. Nichols in 1893

SECOND SERIES, VOL. 69, NOS. 1 AND 2 JANUARY 1 AND 15, 1946

Fast Neutron Energy Absorption in Gases, Walls, and Tissue

PAUL C. AEBERSOLD,* *Radiation Laboratory, Department of Physics, University of California, Berkeley, California*
AND
GLADYS A. ANSLOW,** *Department of Physics, Smith College, Northampton, Massachusetts*
(Received August 12, 1945)

The ionization produced by a collimated beam of fast neutrons, filtered for gamma-rays, resulting from neutron collisions in various hydrogenous and non-hydrogenous gases at pressures ranging from 3 mm to 3 atmospheres or resulting from collisions in various hydrogenous and non-hydrogenous wall materials has been measured in ionization chambers of various types. In large wire-defined gas-walled chambers the ionizing particles are the recoiling gas nuclei. The long range protons of hydrogenous gases expend part of their energy in the walls of the container at ordinary pressures; hence their ionization-pressure curves are quasi-parabolic, becoming linear at higher pressures in accordance with theoretical predictions. The ionization-pressure curves for non-hydrogenous gases are linear except at low pressures. The limiting pressures at which linearity sets in lead to maximum values of the range and energy of the recoiling nuclei and indicate that in the beam of the 37-inch Berkeley cyclotron 5-Mev neutrons predominate. The slopes of the linear portions of the $i-p$ curves permit the calculation of the rate, E_i, at which energy is transferred from the neutron beam to nuclear constituents of the gas. The component of the ionization resulting from gamma-rays, produced in the target and in the walls of the collimator and chamber, was found less than 1 percent in hydrogenous gases and only 2–6 percent in other gases. From the rate of energy transfer and the neutron energy flux an approximate mean value of the $n-p$ cross section for neutron energy distribution of the beam was calculated; also the lower limits of similar cross sections for other nuclei have been estimated, these values containing both the scattering cross sections and those due to neutron absorption followed by disintegrations. In thimble chambers with 1-cm and in cylindrical chambers with 2-mm wall separations, the ionization results in large part from the recoiling wall nuclei. Ranges and energies of the heavier recoiling wall nuclei are indicated by the limiting pressures revealed in $i-p$ curves. The gamma-ray percentage is greater than in large volumed chambers. Neutron responses from most non-hydrogenous walls are practically independent of wall material. The excess response from hydrogenous walls is proportional to proton content. From the E_i values measured in large chambers the energies absorbed per g of various biological substances and of hydrogenous and non-hydrogenous wall materials have been calculated, and (1) predict the respective responses measured in thimble chambers and (2) indicate that the energy absorption per g of tissue must be similar to that for a wall material like amber. Finally, analysis of the relative x-ray and neutron energy absorptions in such materials yields a factor $k_n>2$, which must be applied to reduce neutron exposures measured in certain hydrogenous-walled chambers to tissue doses.

INTRODUCTION

IN a review[1] of the physiological effects of neutron rays on various types of biological media Aebersold and Lawrence included a discussion of the ionization measurements utilized in dosimetry and referred to an extended study of the ionization effects obtained in gas-filled chambers under varied operating conditions, i.e., with an assortment of sizes, wall materials, and gases at pressures ranging from 3 mm of Hg to 3 atmospheres, when exposed to a collimated beam

* At present with Manhattan Engineer District Project, Los Alamos, New Mexico.
** At University of California during sabbatical leave from Smith College.
[1] P. C. Aebersold and J. H. Lawrence, Ann. Rev. Physiol. 4, 25 (1942).

of fast neutrons produced under standard operating conditions in the 37-inch Berkeley cyclotron. The results of this investigation permitted the calibration of the thimble chambers commonly employed in biological experiments at this laboratory, giving a measure of the energy absorbed per gram of biological material, and hence an estimate of the relative effectiveness of neutron and x-ray irradiation of these materials.

The theoretical analysis of the ionization measurements is of considerable importance in pure nuclear physics, since average values of fast neutron cross sections for the nuclei of the various gases employed may be calculated from the ionization measurements taken in large gas-walled chambers, and the ranges and hence the energies of the various recoil nuclei released from the wall materials are revealed in the results obtained with small chambers. Preliminary descriptions of these experiments, which were performed at the University of California in 1938–1939, have been presented before the American Physical Society.[2] Publication of complete details has been delayed by the pressure of the activities of at least one of the authors in war research.

Three groups of experiments were undertaken. In the first a large ionization chamber (Type I) was used with gas-like walls and with dimensions so chosen that at normal pressures the ranges of recoil nuclei scattered in elastic collisions were less than the chamber dimensions. Numerous gases at wide ranges of pressures were employed. At the higher pressures all recoiling nuclei responsible for the measured ionization were released from the gas itself. In the second group very small chambers (Type II) with walls of hydrogeneous and of non-hydrogenous materials were employed, such that at normal pressures most of the neutron ionization was effected by nuclei released from the walls, the ranges of the recoil protons far exceeding the chamber dimensions. In the third group of chambers (Type III) intermediate sizes with solid walls were filled with selected gases under varying pressure conditions and the results used to interpret the measurements obtained with large and small chambers. The ionization occurring in the first type of chamber may be characterized as resulting from the "gas effect," with the second type as from the "wall effect," and with the third as from combined gas and wall effects.

[2] P. C. Aebersold and G. A. Anslow, Phys. Rev. **55**, 680, 1134 (1939).

THEORETICAL CONSIDERATIONS

Fast Neutron Energy Spent in Ionization

In all chambers ionizing particles are released from the walls and the contained gas either by elastic or inelastic scattering of nuclei in neutron collisions, by nuclear disintegrations following neutron absorption, or by electron emission consequent to gamma-ray absorption in the walls. Since biologically important light nuclei, with the exception of nitrogen, have very small cross sections for neutron absorption, in the following treatment this effect may be neglected and only introduced in particular problems involving nitrogen. Moreover, since inelastic collisions cannot occur with protons and are not considered very probable for other biologically important nuclei, most of the neutron energy must be spent during elastic scattering processes.

The Gas Effect

The energy transferred to the gas may be evaluated by considering the effects within a small test volume situated within a large volume of a gas undergoing irradiation, the distances of the surface of the test volume from the outside boundary being greater than the range of any of the ionizing particles. A condition of secondary particle equilibrium exists within such a volume, even though the ranges of the ionizing particles exceed its dimensions, for the energy expended outside the test volume by particles originating within it is compensated by the energy expended within the volume by those particles which originate outside but traverse it.

In general a neutron beam, particularly that from a D—Be source, is complex in its energy distribution. The evaluation of the transferred energy is correspondingly involved. To accomplish this, consider the effect in such a test volume of a homogeneous beam of $N(k)$ neutron with energy $E(k)$ on the $\sum_j N_{T,p} n_j$ nuclei in unit volume of the gas, k being the wave number of the neutrons and $N_{T,p}$ the number of molecules per cc at temperature T and pressure p, each

containing n_j atoms of type j. Both the neutron elastic collision cross section per unit solid angle, $\sigma_j(k, \theta)$, and the fraction of the neutron energy, $f_j(\theta)$, transferred during collisions depend on the scattering angle, θ; hence, the mean fraction of energy transferred per atomic nucleus per incident neutron is given by an energy conversion coefficient

$$K_j(k) = \langle 4\pi\sigma_j(k, \theta) f_j(\theta)\rangle_{Av}$$

$$= 16\pi \frac{m_n m_j}{(m_n+m_j)^2} \langle \sigma_j(k, \theta) \sin^2 \tfrac{1}{2}\theta\rangle_{Av}, \quad (1)$$

since

$$f_j(\theta) = \frac{4m_n m_j}{(m_n+m_j)^2} \sin^2 \tfrac{1}{2}\theta. \quad (2)$$

The neutron energy transferred to the ionizing gas particles which produce $I_{G,G}(k)$‡ ions per cc of gas G with a mean expenditure of energy, W_G, per ion pair is, writing $Q(k) = N(k)\cdot E(k)$ for the energy flux of the $N(k)$ neutrons,

$$W_G I_{G,G}(k) = N_{T,p} Q(k) \sum_j n_j K_j(k), \quad (3)$$

an expression differing from that stated by Gray and Read[3] only through the recognition of the varying asymmetrical character of the scattering cross sections with neutron energy. Since $N_{T,p} = N_{T,760} p/760$, it is obvious that in such a test volume the ionization density is a linear function of the pressure p.

The "gas-walled" chamber utilized in these experiments realized these ideal conditions when filled with non-hydrogenous gases, but in most hydrogenous gases the recoil protons have ranges in excess of the dimensions of the outside shield, as do the faster nuclei in non-hydrogenous gases at low pressures. Under these conditions only a portion of the energy of the recoil particles is utilized in producing ions in the gas, the rest being expended in the walls, the fraction utilized being approximately the mean ratio, $\bar{r}_j(g, k, \theta)p$, of the path lengths within the confining chamber to the corresponding ranges of particles at that gas pressure, this ratio being a function of the geometry, g, of the chamber, the neutron energy and scattering angle, and of the pressure. Under these conditions the energy spent in ionization per cc of the gas

$$W_G I_{G,G}(k) = N_{T,760}(p/760)^2 Q(k) \times \sum_j n_j K_j(k) \bar{r}_j(g, k, \theta) \quad (4)$$

is a quadratic function of the pressure and consequently ionization-pressure curves are parabolic.

Because of the distribution in energy of the neutron beam and the various scattering angles, the range of the recoil nuclei must vary widely. For each energy of recoil particles of type j there is a transition pressure $p_{G(j)}$ of the gas G, at which the limiting dimension of the solid container equals the range R_j. At higher pressures the ionization-pressure curve is linear and the energy expenditure equation is

$$W_G I_{G,G}(k) = \frac{N_{T,760}}{760} Q(k) \sum_j n_j K_j(k) \times [(p^2_{G(j)}/760)(R_j)\bar{r}_j + \{p - p_{G(j)}(R_j)\}], \quad (5)$$

and the slope of the ionization-pressure curve

$$\frac{d}{dp}[W_G I_{G,G}(k)] = \frac{N_{T,760}}{760} Q(k) \sum_j n_j K_j(k), \quad p > p_{G(j)} \quad (6)$$

has the same magnitude as the corresponding expression obtainable from Eq. (3), which expresses the ideal conditions. This correspondence is achieved at pressures of a few cm of Hg in non-hydrogenous gases, since the ranges of the recoil particles in these gases seldom exceed a few mm at atmospheric pressure. In hydrogenous gases, on the other hand, the long ranges of recoil protons at normal pressures necessitate the use of several atmospheres of pressure before this condition is realized.

Finally, the complexity in the energy distribution of the neutron beam demands that all these expressions, (2)–(6), be summed for neutrons of various wave numbers, k. For example,

$$\frac{d}{dp}[W_G \sum_k I_{G,G}(k)] = \frac{N_{T,760}}{760} \sum_k \sum_j \times Q(k) n_j K_j(k), \quad p > p_{G(j)}, \quad (6')$$

which indicates for the rate E_m, at which the

‡ $I_{G,G}$ represents the ionization in gas G surrounded by a wall of G. $I_{A,G}$ represents the ionization in gas G surrounded by a wall of material A.

[3] L. H. Gray and J. Read, Nature **144**, 439 (1939).

neutron energy is transferred per molecule of the gas

$$E_m=\frac{d}{dN}[W_G \sum_k I_{G,G}(k)]$$
$$=\frac{760}{N_{T,760}}\frac{d}{dp}[W_G \sum_k I_{G,G}(k)]_{,\ p>p_{G(j)}}$$
$$=\sum_k \sum_j Q(k) n_j K_j(k), \quad (7)$$

a corresponding expression holding for E_j, the rate of energy absorption per atom. The evaluation of these latter quantities, E_m and E_j, make possible the interpretation of the effect of fast neutron irradiation on organic material.

Fast Neutron Cross Sections

The determination of E_j and hence of the energy conversion coefficient, $K_j(k)$, leads under particular conditions to the evaluation of the mean value over all scattering angles of fast neutron cross sections. To accomplish this the energy content of the beam must be known and a theoretical expression for $\sigma_j(k, \theta)$, such as that given by Placzek and Bethe[4] in their development of the continuum theory of the complex nucleus, must be employed. If the scattering angular distributions are symmetrical in space in the center of mass system, as is nearly true for $n-p$ cross sections except at very high energies,

$$\bar{\sigma}_j=4\pi\langle\sigma_j(k, \theta)\rangle_{Av}=\frac{(m_n+m_j)^2}{2m_n m_j}K_j(k), \quad (8)$$

$\bar{\sigma}_j$ being the mean cross section weighted for the energy distribution of the neutron beam. However, angular distributions are usually distinctly asymmetrical,[5] mainly in the forward direction at high energies, and (8) will give values greater than the mean cross sections averaged over all scattering angles as well as neutron energies, since

$$\langle\sigma_j(k, \theta)\sin^2\tfrac{1}{2}\theta\rangle_{Av}<\langle\sigma_j(k, \theta)\rangle_{Av}. \quad (9)$$

The Wall Effects

As already stated, the energy released by ionizing particles from the chamber walls results from neutron collisions and gamma-ray absorption. The neutron energy transferred during elastic collisions decreases with increasing mass of the nucleus, (Eq. (2)); hence the effect of the recoil nuclei must be treated in two categories: (1) those with ranges in excess of the chamber dimensions, such as protons and C, O, and N nuclei at low pressures in small chambers and (2) those with ranges less than the chamber dimensions, the heavier nuclei at normal gas pressures. Although the ionization resulting from the latter group is small, it is a sensible portion of that produced in small chambers and cannot be neglected. It is difficult to evaluate accurately since the nuclei released at different levels within the chamber walls travel correspondingly different distances within the chamber. In chambers with wall separation of about a cm, as the experiments to be described indicate, the effect may be neglected at normal pressures since the energy lost by C, O, and other heavy recoil particles to the gas is nearly compensated by the energy lost in the walls by recoiling gas nuclei.

Gamma-radiation of quite high energy is created in the target with the production of fast neutrons or arises from scattering and absorption of fast and slow neutrons by surrounding materials. The secondary electrons released from the walls hence have much longer ranges than those of the recoil nuclei. It is possible to differentiate the resulting ionization in Type I chambers, and thus to evaluate it for the other chambers, since the neutron ionization varies parabolically with pressure at low pressures but linearly at high pressures and the gamma-ray ionization varies linearly at all pressures.

As Gray[6] has shown, the kinetic energy Q_A of all fast moving particles released from unit volume of a medium A, which cross a cavity filled with gas G, producing $I_{A,G}$ ions per cc, is given by the equation

$$Q_A=I_{A,G}W_G(S_A/S_G), \quad (10)$$

or

$$Q_A=I_{A,G}W_G(N_A s_A/N_G s_G), \quad (11)$$

S_A, S_G, and s_A, s_G representing the stopping powers of the wall and of the gas per cc and per molecule, respectively. The dependence of the magnitudes of these stopping powers and also of

[4] G. Placzek and H. A. Bethe, Phys. Rev. **57**, 1075 (1941).

[5] H. Aoki, Phys. Rev. **55**, 795 (1939); S. Kikuchi, H. Aoki, and I. Wakatuki, Phys. Rev. **55**, 1264 (1939); T. Wakatuki and S. Kikuchi, Proc. Phys. Math. Soc. Jap. **21**, 656 (1939).

[6] L. H. Gray, Proc. Roy. Soc. **A156**, 578 (1936).

W_G upon the mass and speed of the ionizing particle have been discussed in detail by Gray.[7]

Writing $I_{A(p),G}$, $I_{A(c),G}$, and $I_{A(e),G}$ for the components of the ionization effected by recoil protons, by heavier recoil nuclei, such as carbon, nitrogen, and oxygen, and by extra-nuclear electrons, respectively, the total ionization which results from the absorption in the wall of neutron energies, $Q_{A(p)}$ and $Q_{A(c)}$, and of gamma-ray ernergy $Q_{A(e)}$, is

$$I_{A,G}=I_{A(p),G}+I_{A(c),G}+I_{A(e),G}$$
$$=\frac{N_{T,p}}{N_A}\left[\frac{Q_{A(p)}}{W_{G(p)}}\frac{s_{G(p)}}{s_{A(p)}}+\frac{Q_{A(c)}}{W_{G(c)}}\frac{s_{G(c)}}{s_{A(c)}}+\frac{Q_{A(e)}}{W_{G(e)}}\frac{s_{G(e)}}{s_{A(e)}}\right];\quad p<p_{G(c)\min} \tag{12}$$

or

$$=\frac{Q_{A(c)}}{W_{G(c)}}+\frac{N_{T,p}}{N_A}\left[\frac{Q_{A(p)}}{W_{G(p)}}\frac{s_{G(p)}}{s_{A(p)}}+\frac{Q_{A(e)}}{W_{G(e)}}\frac{s_{G(e)}}{s_{A(e)}}\right].\quad p>p_{G(c)\max}. \tag{12'}$$

The corresponding ionization-pressure curves will inflect in the region of the pressures $p_{G(c)}$, for which the limiting chamber dimension is the range of some of the heavier recoil nuclei. Since there are usually several types of such nuclei in wall materials and there is wide scattering, the energies and hence the ranges of the nuclei must vary widely. Consequently, the slope of the ionization-pressure curve will start to decrease at a pressure $p_{G(c)\min}$, corresponding to short ranges and continue to decrease up to $p_{G(c)\max}$ defining long ranges.

Since the measured ionization I_G is the sum of that produced by the wall particles and the recoiling gas nuclei, $I_{A,G}+\sum I_{G,G}(k)$, there will be inflections of this curve for each of the transition pressures, $p_{G(j)}$. From these the ranges of the gas nuclei may be calculated.

Identification of the Gamma-Ray and Neutron Components

Several series of measurements are necessary to separate gamma-ray from the various neutron components of the ionization measured. In the experiments of Type I, chambers with non-hydrogenous walls are filled with hydrogen at low pressures. The measured ionization may be written

$$I_{A,G}=a+bp+cp^2, \tag{13}$$

where

$$a=\frac{Q_{A(c)}}{W_{G(c)}};\quad b=\frac{N_{T,760}}{760}\frac{Q_{A(e)}}{W_{G(e)}}\frac{s_{G(e)}}{N_A s_{A(e)}},$$

and

$$c=\frac{N_{T,760}}{(760)^2}\sum_k\sum_j\frac{Q(k)n_j}{W_{G(j)}}K_j(k)\bar{r}_j(g,k,\theta).$$

Accordingly, observations taken at various low pressures permit the evaluation of the constants, a, b, and c, identifying the gamma-ray (b) and neutron components of the gas (c) and wall (a) effects.

Since the gamma-ray ionization produced from the same wall in different gases at the same pressures are related as

$$\frac{I_{A,G}}{I_{A,G'}}=\frac{b}{b'}=\frac{s_{G(e)}}{s_{G'(e)}}\times\frac{W_{G'}}{W_G}, \tag{14}$$

the gamma-ray component in other gases may be calculated from the hydrogen determination. Values of stopping powers for gamma-ray produced electrons, not those in the literature for alpha-rays, must be used. This necessitated measurements of these stopping powers in various gases which were irradiated by a pure gamma-ray source with an energy content similar to that encountered in the neutron experiments.

At higher pressures, $p_{G(j)}$, in any gas, both the gamma-ray and the neutron "gas-effect" increase linearly with pressure, and the neutron component of the non-hydrogenous "wall effect" does not appear in the equation

$$\frac{dI_G}{dp}=\frac{d}{dp}[\bar{I}_{A,G(e)}]+\frac{d}{dp}[\textstyle\sum_k I_{G,G}(k)]. \tag{15}$$

By using in this equation values obtained for gamma-ray components through the preceding equation, neutron "gas effects" are finally derived, the quantities desired for the interpretation of biological measurements and for the calculation of fast neutron cross sections.

If the chamber walls contain hydrogen, an auxiliary measurement must be made, for the method above does not differentiate between proton and gamma-ray components in the "wall

[7] L. H. Gray, Proc. Camb. Phil. Soc. **40**, 72 (1944).

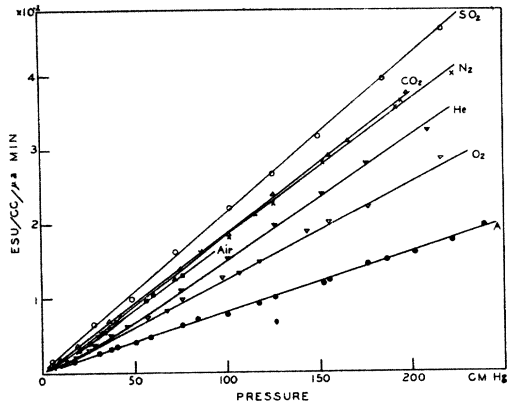

FIG. 1. Ionization-pressure curves for non-hydrogenous gases in gas-walled chamber, linear at normal pressures. Ranges of recoil particles < chamber dimensions.

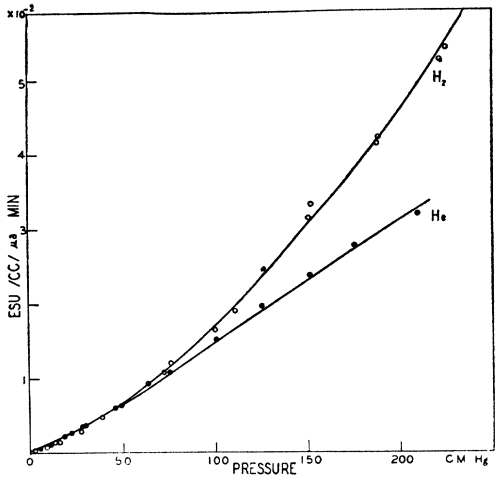

FIG. 2. Ionization in hydrogen and in helium. Ranges of recoil protons > chamber dimensions at all pressures employed. Ranges of alpha-particles < chamber dimensions at pressures > 70 cm.

effect." An extensive study[8] of the relative gamma-ray ionizations resulting in various hydrogenous and non-hydrogenous walled chambers filled with the same gas has shown that the gamma-ray effect in light wall materials, such as carbon, bakelite, and amber, are practically the same. Hence comparative measurements with a carbon chamber may be used to separate gamma-ray and neutron ionization effects in chambers with hydrogenous walls.

EXPERIMENTAL PROCEDURE

The Neutron Source

The neutron source used in the early biological experiments of this laboratory[8] was employed. A beryllium target in the 37-inch cyclotron of Lawrence and Cooksey[9] was bombarded by 8-Mev deuterons and the measurements were made at the exit of the collimating arrangement described by Aebersold,[8] which gives a neutron beam in the forward direction of the deuteron beam. This arrangement localizes the effect of the fast neutrons to a sharply defined region and quite well suppresses gamma-ray effects. It does not absorb slow neutrons other than by the large masses of the material of the collimator.

The Ionization Chambers

A gas-walled chamber (Group I) was formed of fine (No. 30) copper wires spaced approximately 7 mm apart to define a cylindrical surface, 3.3 cm long and 4 cm in diameter, the ends being formed by meshing wires with the same spacing, thus forming a volume of about 66 cc with a 96 percent gas-walled surface. The collecting electrode, 3 mm in diam. and 4.5 cm long was mounted along the axis of the cylinder, and the lead to this electrode was protected against the collection of ions in the space between the shield and the chamber by a cylindrical brass guard which surrounded the amber insulating plug and was in contact with the outer shield. This chamber was housed in a large brass cylindrical shield, leaving 10 cm between the front faces of the shield and the chamber, 5 cm between their rear faces, and 5 cm between their cylindrical surfaces, distances adequate to provide inside the chamber the conditions of secondary particle equilibrium discussed earlier in this paper. The front face of the shield was placed in contact with the aperture of the neutron collimating cones, so that the neutron beam was directed along the length of the ionization chamber. The center of the chamber was approximately 85 cm from the neutron source.

TABLE I. Magnitudes of Jaffé constant "c."

Gas	O_2, CH_4, C_2H_4, C_2H_6, C_3H_8, C_4H_{10}, H_2S, NH_3	SO_2, C_2H_2	CO_2
c	10^{-4}	10^{-5}	3×10^{-6}

[8] P. C. Aebersold, Phys. Rev. 56, 714 (1939).
[9] E. O. Lawrence and D. Cooksey, Phys. Rev. 50, 1131 (1936).

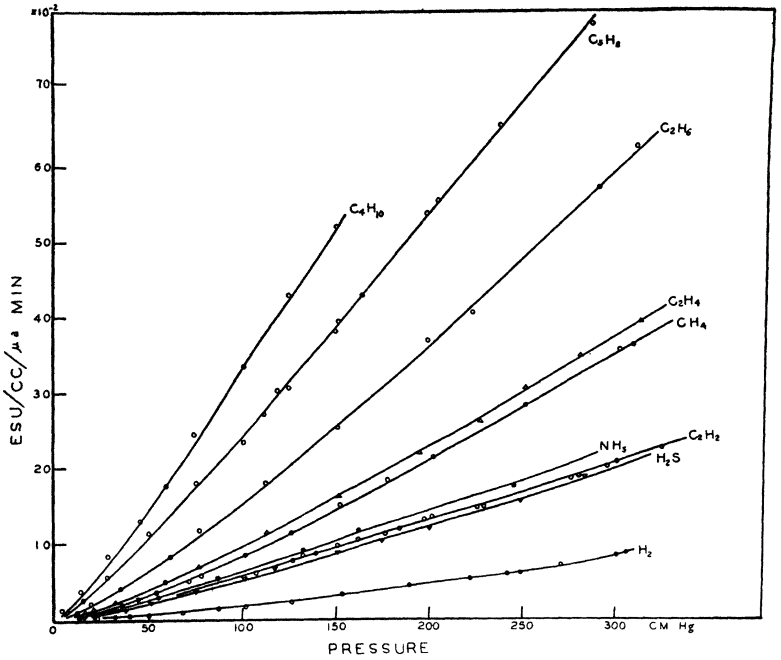

FIG. 3. Ionization-pressure curves in hydrogenous gases. Transition pressures occur in H_2S, C_2H_2, CH_4, C_2H_4, C_2H_6, C_3H_8, C_4H_{10} at 240, 240, 275, 200, 190, 130, and 100 cm, respectively.

Type II chambers were of two kinds, the thimble chambers, described by Aebersold[8] with C, brass, Cd, Sn, Pb, Bakelite, and Amber walls, and "cylindrical" chambers with C and celluloid walls.[10] The latter consist of an inner cylindrical electrode of the material, 1.22 cm in diam. and 5.0 cm long, held concentrically inside a tube of the same material of 1.43 cm inside diam. of an amber plug. To protect the brass lead of the center electrode from the collection of ions, it is mounted inside a concentric brass shielding tube. The effective volume of the chamber is 2.15 cc. To render the celluloid surfaces conductive they were sparsely covered with powdered graphite. Neutron beams were directed across the Type II chambers, normal to their axes. In the thimble chambers the longest path available to recoil wall particles is the 1-cm diameter, and in the cylindrical chambers this limiting distance is 0.74 cm, the width of the plane which is tangent to the outer surface of the inner electrode and is bounded by its intersections with the outer cylinder.

[10] Chambers of various other wall materials were constructed, but the measurements taken are too limited in extent to report at this time. The Bakelite material was that used in the manufacture of Victoreen chambers.

The Measurements

Ionization currents were measured by a null method with an FP54 electrometer tube amplifier, the tube and high resistors being housed in an evacuated chamber. To avoid any effect from the strong magnetic field of the cyclotron, the tube was magnetically shielded by a concentric iron cylinder, also housed inside the chamber, which was located about 60 cm from the ionization chamber, practically outside of the magnetic field. Connection between the control grid and the collecting electrode of the ionization chamber was made by a fine wire strung through amber insulators supported in an evacuated shielding tube. To protect the observer from harmful biological effects the measuring circuit was placed outside the 30-inch water walls which surround the cyclotron. To eliminate radio frequency effects the entire circuit assembly with its leads was housed in a continuous copper shield, using a common ground; to dampen out this pick-up on the high voltage lead to the ionization chamber a filter was introduced just outside the chamber. Finally, all zero readings were taken with the oscillators in operation, the test of

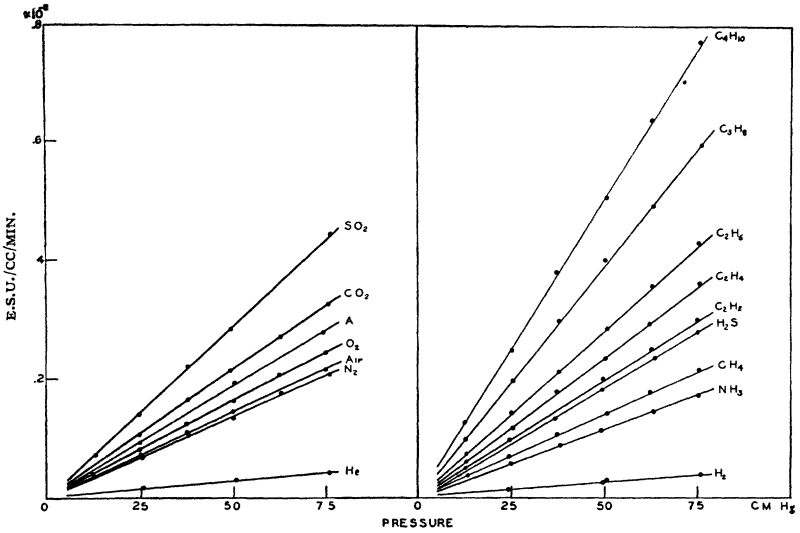

FIG. 4. Gamma-ray ionization curves for 100-cc chamber, showing validity of Bragg-Gray relation (ionization linear with pressure and proportional to stopping power of gas). Relative gamma-ray responses compared with those for neutron ionization (Figs. 1 and 3) indicate the distinctly different relative magnitudes of the energy absorbed by the ionizing particles, electrons or nuclei, respectively.

adequate shielding being identical circuit calibrations with or without oscillator operation.

With the large chambers ionization currents were measured in sixteen gases, including air, at pressures ranging from 3 mm of Hg to 4 atmospheres in hydrogenous gases and to only 2 atmospheres in non-hydrogenous gases. The complete results for only the "gas-walled" chamber will be quoted, those with the 100-cc and 500-cc brass chambers being used for interpretative purposes. With the small chambers currents were read in a few of these two types of gases, the maximum pressures being one or two atmospheres.

The neutron output for a particular deuteron current, maintained between 25 and 30μamp., was kept steady during measurements, its constancy being checked at frequent intervals by using as monitor the ionization produced in the 100-cc brass chamber when filled with air at atmospheric pressure. All ionization values were reduced to the number of electrostatic units of charge associated with ions of one kind produced per cc per μamp. min. of deuteron charge. It was found that if any of the principal operating conditions of the cyclotron varied, such as the strength of the magnetic field or the deflector voltage, a simultaneous variation occurred in the neutron output. Hence, all sets of readings reported in this paper were taken within short intervals of time during which the operating conditions remained nearly constant, several independent sets of readings being taken for each gas, results agreeing within 2–3 percent.

Since the ionization produced by recoil nuclei is columnar and very dense, ionic recombinations occurred, particularly at high pressures; accordingly corrections were made to the measured values of the ionization at various voltages according to the theory of Jaffé,[11] using the method of Zanstra.[12] These corrections were not made in the earlier reported results, nor was recombination taken into account in the similar early measurements of Bonner.[13] With the large chambers a voltage-supply which gave 3250 volts with 400-volt intervals was employed for all but the lower pressures, for which batteries were substituted, since they permitted smaller voltage intervals. With the small chambers batteries were adequate except for the highest pressures. In the application of the Jaffé-Zanstra formula to the results obtained with the gas-walled chamber the average field intensity in a region within one cm of the cylindrical walls of

[11] G. Jaffé, Ann. de Physique **42**, 303 (1913).
[12] H. Zanstra, Physica **2**, 817 (1935).
[13] T. W. Bonner, Phys. Rev. **45**, 101 (1934).

the chamber was used, since calculations indicate that the field varies only slightly in this region and that the volume of the region is such that about $\frac{3}{4}$ of the ions are produced within it. With 3250 volts between the walls and the collecting electrode the field in this region was about 1000 volts per cm in the wire chamber and about $\frac{1}{3}$ this value in the 500-cm solid-walled chamber. Closer to the central collecting electrode the fields were naturally much larger.

The value of the Hankel function employed in a reduction was obtained from coefficient c, itself determined by the Zanstra method. This coefficient has been determined previously for a limited number of gases, for air by Zanstra[12] and for He, N, Ar, and Ne by Clay and Kwieser,[14] the present observations demanding the same values of c for their reduction. The approximate values of c obtained for other gases are listed in Table I. Collection was so nearly complete in hydrogen, even at the highest pressure, no value of c was obtained. The smaller the value of c, the more likely are recombinations under identical pressure and electric field conditions.

DISCUSSION OF RESULTS

The gases studied with the "gas-walled" chamber fall into two groups: non-hydrogenous gases, in which recoil nuclei have relatively short ranges; and hydrogenous gases, in which the recoil protons have relatively long ranges, H_2, CH_4, C_2H_4, C_2H_6, C_3H_8, C_4H_{10}, C_2H_2, H_2S, and NH_3. In Fig. 1 are shown the ionization-pressure curves, corrected for ionic recombinations, of the non-hydrogenous group, which except for that of He are linear beyond 5 cm mercury pressure, indicating that at all but very low pressures the conditions necessary for secondary particle equilibrium exist. Because of the longer range of He nuclei and the smaller stopping power of the gas, this equilibrium condition is not fulfilled in He at pressures less than 70 cm, the ionization-pressure curve being quasi-parabolic at lower pressures, as is evident in Fig. 2. The diagram also depicts the parabolic $i-p$ conditions in H_2, in which gas the proton ranges are so long that the equilibrium condition was not attained even at the maximum pressure employed.

The corresponding $i-p$ curves obtained with the hydrogenous gases are shown in Fig. 3. At the lower pressures all these curves are quasi-parabolic. For the gases with the greater stopping powers the curves become linear at approximately one atmosphere pressure; as the stopping powers decrease the transition pressures increase, occurring at about 3 atmospheres for CH_4. The mean value of the normal range in air (24.0 ± 0.95 cm) of these long range protons, obtained from the curves for H_2S, C_2H_2, CH_4, C_2H_4, C_2H_6, and C_3H_8, indicates that these protons and hence many of the neutrons have energies of about 5.0 Mev (estimated from the Livingston and

TABLE II. Molecular stopping powers for fast electrons released from brass by gamma-rays from Ra.

Gas	Ionization per cc relative to air	Total ionization relative to air (quoted from alpha-particle measurements)	Molecular stopping powers relative to air for fast electrons	Molecular stopping powers relative to air for alpha-particles (quoted)
H_2	0.170	0.99 (1, 2)	0.17	0.21 (5)
He	0.192	1.148 (3)	0.16	0.175 (6)
N_2	0.94	0.98 (3)	0.96	0.990 (5)
O_2	1.13	1.10 (4)	1.03	1.060 (5)
CO_2	1.49	0.996 (4)	1.50	1.53 (7)
SO_2	2.00	1.03 (1)	1.93	1.87 (8)
A	1.31	1.38 (3)	0.96	0.97 (6)
CH_4	0.97	1.173 (1)	0.82	0.88 (11)
C_2H_2	1.37	1.265(1)	1.08	1.12 (11)
C_2H_4	1.62	1.22 (1)	1.33	1.34 (11)
C_2H_6	1.93	1.30) (1)	1.47	1.53 (11)
C_3H_8	2.58	(1.31)	2.01	(2.09) (11) (13)
C_4H_{10}	3.47	(1.33)	2.61	(2.72) (11) (13)
H_2S	1.29	(1.27) (9, 10)	1.01	(1.12) (11) (13)
NH_3	0.80	0.90 (1)	0.89	0.82 (11) (12)

[14] J. Clay and M. Kwieser, Physica **5**, 724 (1938).

TABLE III. Total ionization and the gamma-ray component; fast neutron energy expended per μ amp. min. of deuteron charge.

Gas	Total ionization in e.s.u. per cc per cm pressure (dI_G/dp)	Gamma-ray component in e.s.u. per cc per cm pressure ($dI_{G(e),G}/dp$)	Percentage due to gamma-radiation	Energy in Mev expended by fast neutrons per molecule (E_m)
H_2	$>4.05\times10^{-4}$	0.70×10^{-6}	<0.17	——
He	1.760	0.79	0.45	3.48×10^{-17}
N_2	1.882	4.09	2.2	4.54
O_2	1.325	4.27	3.6	2.82
CO_2	1.893	7.09	3.7	4.37
SO_2	2.172	8.26	3.9	5.06
A	0.772	3.98	5.8	1.33
CH_4	13.61	3.98	0.29	26.90
C_2H_2	8.33	5.65	0.68	15.50
C_2H_4	13.30	6.93	0.45	28.56
C_2H_6	23.20	8.06	0.35	41.19
C_3H_8	30.53	10.38	0.34	54.82
C_4H_{10}	37.83	14.29	0.38	68.11
H_2S	7.98	5.83	0.73	14.62
NH_3	8.12	3.29	0.40	21.01
Air	1.669	4.16	2.5	3.96

TABLE IV. Effect of chamber dimensions on total ionization and on percentage due to gamma-rays.

Chamber Type	Chamber Wall	Ratio surface area to volume	Distance from target	Gamma-ray percentage in air	CO_2	A	CH_4	Ionization in normal air in e.s.u./cc/μ amp. min. $\times 10^2$ (a) measured	(b) neutron component at 74 cm from target
wire	gas	0.36	85 cm	2.5	3.5	5.8	0.29	1.30	1.66
100-cc	brass	0.81	80	3.9	5.4		0.50	1.51	1.68
500-cc	brass	1.42	80	8.0	11.0	21.2	3.7	1.58	1.69
thimble	brass	5.0	74	20?	30?			2.04	1.64
thimble	carbon	5.0	74	20?	30?			1.96	1.57

Bethe range curves).[15] The helium results discussed above indicate neutron energies of at least 4.5 Mev.

Separation of the Gamma-Ray and Neutron Components

Since 8-Mev deuterons on beryllium may release 12 Mev of energy, these 5-Mev neutrons must be accompanied by strong gamma-radiation, much of which was suppressed from the beam by the lead filter. Before estimating the portion of the response of the different gases in the various chambers caused by gamma-radiation, the applicability of the Bragg-Gray relationship (Eqs. (10) and (14)) was tested by use of the 100-cc and the 500-cc brass chambers and a 1.07-mc Ra standard with a 1-mm Pb filter. In each gas the resulting ionization, Fig. 4, appeared to be linear with gas pressure, indicating that even in the gases with the greatest stopping powers the high energy electrons liberated from the brass walls completely crossed the chamber. Gamma-ray stopping powers were calculated from the slopes of the ionization-pressure curves and are of the same order of magnitude as, though not equal to, the values measured in alpha-particle stopping, in agreement with the theory that stopping powers for fast electrons are relativity functions of their velocity and for heavy particles are effected by the difficulty they experience in producing K-electron ionization.[16]

For the calculations, values of W_G, or of relative ionizations W_G/W_{air}, produced by high energy electrons, protons, and other recoil nuclei, were required. As Gray[7] has pointed out, the mean energy expended in ionization varies not only with the nature of the ionizing particle, i.e., with its mass and cross section, but also with its velocity. At low energies magnitudes of W_G increase rapidly as the energy of the ionizing particle decreases; at high energies magnitudes are practically constant, in air being approximately 35.1 ev for 6–8-Mev alpha-particles, 36.0 ev for 1–8 Mev protons, and 32.5 ev for high energy electrons. Moreover, at these high energies relative ionization magnitudes appear to be nearly independent of the nature of the ionizing particle, though at low energies values are functions of the velocity of the particle and also of the gas concerned. At high energies the ionization relative to air for H_2, N_2, D_2, CO_2, and SO_2 is practically unity, a value frequently employed in energy-loss calculations, but lies between 1.2 and 1.3 for the hydrocarbon and monatomic gases. No investigations are recorded giving values of W_G for the C, N, O, S, and A recoil nuclei, which were ionizing agents in some of the gases concerned, but since C, O, and N particles take from the neutrons about one-quarter of the energy imparted to recoil protons, and S and A particles less than one-eighth, corresponding W values must be fairly large, certainly as large as

TABLE V. Percentage decrease caused by magnetic field on ionization produced by gamma-radiation.

Chamber	Diameter	Percentage decrease with chamber located (a) at collimator exit	(b) adjacent to magnet pole
Shield of wire mesh	14.0 cm	30	50
500-cc	7.6	5	32
100-cc	3.3	1	4
Thimble	1.0	none	1

[15] M. S. Livingston and H. A. Bethe, Rev. Mod. Phys. 9, 245 (1937).
[16] M. S. Livingston and H. A. Bethe, Rev. Mod. Phys. 9, 263–265 (1937).

that obtained with 1–2-Mev alpha-particles, namely 38.0 ev in air. This value was used in the calculations which involved ionizations by the heavier recoil nuclei, introducing uncertainties of 2–3 percent in resulting magnitudes, smaller uncertainties being introduced by using 32.5 ev for the electron, 36.0 ev for proton, and 35.6 ev for alpha-particle ionizations. In addition relative ionizations in the various gases were assumed the same for all these particles, for their energies were sufficiently high to warrant the assumption. The resulting values of fast electron stopping powers are listed in Table II together with the quantities used in their calculation and with mean values of alpha-particle stopping powers.[17]

The ionization produced by the neutron source in hydrogen at low pressures with "gas-walled" chambers was carefully measured and from the values obtained at pressures less than 3 cm mercury the value of "a" in Eq. (13) was determined as 0.678×10^{-6} e.s.u./cc/μ amp. min. per cm pressure. From these measurements and the values of W_G obtained from Table II the gamma-ray component of the ionization produced in the other gases was calculated through Eq. (14), the resulting values of $dI_{G(e)}/dp$, accurate to 20–30 percent, being listed in Table III.

The table also includes the experimental values of dI_G/dp (total) (with less than 2 percent probable error in the measurements), and the percentages of the total ionization attributable to gamma-rays at pressures in excess of the respective limiting pressures. It is apparent that the gamma-ray component of the measured ionization varies from less than 1 percent of the total in gases containing hydrogen and helium to 2–6 percent in gases containing only heavier particles.

Similar calculations from low pressure hydrogen curves in the solid-walled brass chambers indicate larger gamma-ray contributions (Table IV), ranging from about 1 percent in hydrogeneous gases to nearly 10 percent in O_2, N_2, and CO_2, and nearly 20 percent in A. But the neutron component, i.e., the "gas effect," is nearly independent of chamber characteristics. The larger gamma-ray contribution in these chambers with smaller dimensions, with a larger ratio of surface area to volume, can be largely attributed to the relatively greater contribution to the ionization from the electrons released from the surfaces. An equally effective cause of the difference may be the deflection of the paths of the light electrons by the magnetic field of the cyclotron, causing a certain percentage of these particles to return to the wall from which they were ejected without passing through the small wire mesh chamber. This hypothesis was tested by measuring the ionization produced by gamma-rays from the Ra standard with the magnetic field on and off. In Table V are tabulated the results obtained with the chambers discussed and also with the small thimble chambers (Type II) used for the study of the wall effect and for neutron dosimetry. In the 100-cc and thimble chambers, in which the walls are fairly close together, the recoiling electrons apparently travel nearly equivalent distances within the chambers on the curved paths imposed by the magnetic field and on the

TABLE VI. Neutron energy transferred per μamp. min. of D charge per atomic nucleus.

Element	Gases used	E_A in Mev per nucleus per μamp. min. of D charge $\times10^{17}$	E_A/E_H
H	CH_4, C_2H_2, C_2H_4, C_2H_6, C_3H_8	6.20±0.07	1.000
He	He	3.48±0.04	0.551
C	CO_2, O_2, C_2H_4, CH_4	1.58±0.02	0.252
N	N_2	2.27±0.03	0.368
O	O_2	1.41±0.02	0.227
S	SO_2, O_2	2.24±0.02	0.360
A	A	1.33±0.02	0.213

[17] Quoted values are from the following sources: (1) A. F. Kovarik and L. W. McKeehan, Bull. Nat. Research Council (1925) No. 51, 72; (2) R. W. Gurney, Proc. Roy. Soc. **A107**, 332 (1925); (3) R. Naidu, Ann. Chim. Phys. **1**, 72 (1934); (4) C. E. Gibson and H. Eyring, Phys. Rev. **30**, 553 (1927); (5) G. I. Harper and E. Solomon, Proc. Roy. Soc. **A127**, 175 (1930); (6) G. Mano, J. Phys. Radium [7] **5**, 628 (1934); (7) C. E. Gibson and E. W. Gardner, Phys. Rev. **30**, 543 (1927); (8) L. F. Bates, Proc. Roy. Soc. **A106**, 622 (1924); (9) W. C. Price, J. Chem. Phys. **4**, 147 (1936); (10) J. C. Morris, Phys. Rev. **32**, 456 (1928); (11) K. Schnieder, Ann. d. Physik **35**, 445 (1939); (12) H. von Trauenberg and K. Phillip, Zeits. f. Physik **5**, 404 (1921); (13) W. H. Bragg, Phil. Mag. **13**, 333 (1907). Values in parentheses are estimated in the absence of experimental determinations; those for relative total ionization by assuming the value of H_2S to be similar to that of C_2H_2 (their ionization potentials are similar); and those of C_3H_8 and C_4H_{10} as intermediate between those of C_2H_6 and C_5H_{12}, quoted in (1). Estimated values of relative stopping powers were obtained by using the Bragg rule that stopping powers are additive.

linear paths followed in the absence of the field, and the gamma-ray ionization is little affected by the magnetic field. But in larger diameter chambers, particularly those constructed with an inner wire collecting chamber, the deflection of the ionizing beta particles materially reduces the gamma-ray ionization.

No tests were made of the effect of the field on the paths of the recoil nuclei released from the walls and gas by neutron irradiation, but the deflecting force on such particles moving in a magnetic field can be only 0.3–2 percent of that on beta-particles of the same energy; hence the effect of the field on neutron ionization must be negligible. This conclusion is confirmed by cloud-chamber photographs taken close to the magnet of the cyclotron.[9]

Rate of Conversion of Neutron Energy by Various Nuclei

From the values listed in the first two columns of Table IV and from Eq. (11) the neutron energy expended in the various gases was calculated by using the W_G values characteristic of the ionizing particle and recalling that in compound gases the neutron energy made available for ionization is distributed between the particles in accordance with Eq. (2), the resulting values being listed in the last column of that table, expressed in terms of E_m, Eq. (7), the rate of absorption of neutron energy per μamp. min. of deuteron charge. In Table VI are given the corresponding values of E_A, the rate of absorption of neutron energy per atomic nucleus, calculated, with the exception of the proton value, either directly from the E_m value of the corresponding gas or as the difference of these values for two gases. From E_C, the weighted mean of the two indicated calculations for carbon, and from the E_m values of the stated hydrocarbons, values of E_H have been calculated, their unweighted mean being quoted. The probable errors of the E_A values result from the errors of the E_m values, themselves propagated from those of WdI_{exp}/dp and the correction for the gamma-ray component of the ionization. From the E_m values of C_4H_{10}, H_2S, and NH_3 together with the E_A values of C, S, and N, respectively, values of E_H, 5.89, 6.04, and 6.13 were obtained but not included in the determination of its probable value because of the uncertainty in the W values of these gases and their relatively large ionic recombinations. Relative values of E_A are also those of the atomic energy conversion coefficients, K_{jk} (Eq. (1)), provided the neutron energy is monochromatic.

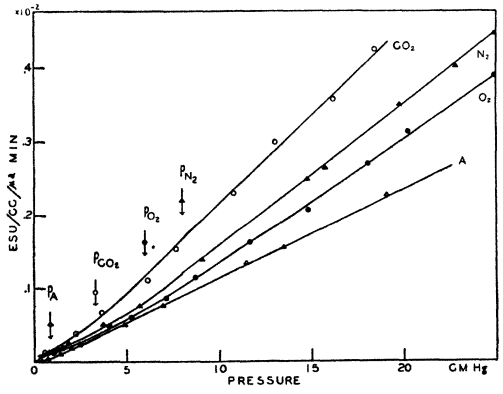

FIG. 5. Transition gas pressures revealed in i–p curves for 100-cc (3.3-cm diam.) brass chamber.

N–p Cross Section (Weighted Mean Value)

As already stated the mean value of the $n-p$ cross section, weighted for the energy distribution of the neutron beam, can be calculated from these values (Eq. (8)), provided the neutron energy flux is known. Lacking a direct measurement of the neutron flux in the beam employed, an approximate value has been calculated by comparing the ionization produced by these D-Be neutrons with that produced by Rn-Be neutrons, measured by Dunning and quoted by Aebersold[8] as 1500 ion pairs per cc of air per sec. at 30 cm from a 1-curie radon beryllium source. In the present experiment 4.28×10^5 ion pairs per μamp. deuteron current were formed per cc of air per sec. at 85 cm from the target; hence the neutron beam created in the 37-inch cyclotron per μamp. min. of 8-Mev deuterons may be considered equivalent to that from a 2.38×10^3 curie Rn-Be source. According to Amaldi, Hafstad, and Tuve[18] 25,000 neutrons per sec. are emitted from the latter source per mc of radon, hence at 85 cm from the source the neutron energy flux per sq. cm is equivalent to that of

[18] E. Amaldi, L. R. Hafstad, and M. A. Tuve, Phys. Rev. 51, 896 (1937).

TABLE VII. Transition gas pressures, and mean ranges and recoil energies.

Transition pressures in cm mercury at 25°C						Ranges and energies at 760 mm and 15°C				
	Chamber and limiting dimension						Range in			
Gas	100-cc brass 3.3 cm	500-cc brass 7.6 cm	Gas-walls 10 cm	Thimble 1.05 cm (calc.)	Cylindrical 2.1 mm (calc.)	Principal recoiling nuclei	gas	air in mm	Energy in Mev of nucleus	neutron
air	7.5	3.5	3	24.8	118	*N*, O	3.2	3.2		
N_2	8.0	4.0		26	124	N	3.3	3.3	1.27	5.07
O_2	6.0	3.0		20	95	O	2.5	2.7	1.10	5.00
CO_2	4.3	2.0		13.5	68	*C*, O	1.89	2.9	1.44	5.14
A	0.5			1.6	8.4	A	0.21	0.20	0.5	5
He		100	70	9 atmos	43 atmos	He	9.2 cm	1.62 cm	2.9	4.55
CH_4			275	36 atmos	172 atmos	H	36 cm	32 cm		
C_2H_4			200	26 atmos	125 atmos	H	26 cm	30 cm		
Mean of C_2H_2, CH_4, C_2H_4, C_2H_6, C_3H_8, and H_2S transition gas pressures lead to H								34 cm		5.0

3.72×10^7 Rn-Be neutrons per μamp. of direct-current. The mean energy of these neutrons, estimated from Dunning's graph[19] for the distribution in range of the forward projected protons and from the energy-range values of Livingston and Bethe, is about 2.5 Mev. Hence the neutron energy flux per μamp. of deuteron current in the beam employed was, approxmately, 9.1×10^7 Mev per min.

The resulting $n-p$ cross section is approximately 1.3×10^{-24} cm^2. From this quantity and the values given in Table VI lower limits of the cross sections of He, C, N, O, S, and A are obtained as 1.1, 1.2, 1.9, 1.4, 4.1, and 3.0×10^{-24} cm^2, respectively. These calculations neglect the effects of asymmetry, but nevertheless indicate that most of the neutron ionization effected by He, C, and O reactions result from elastic collisions, and that 30–40 percent of the N effects must result from disintegrations. The magnitudes obtained for the heavier nuclei may be relatively small since the 38-ev value used for W_G in the E_m calculations may have been too low. Since the ionization curves indicated that many 5-Mev neutrons as well as neutrons with lower energies and possibly some with higher energies were in the beam, the weighted mean cross sections must be quite different from values measured for monoenergetic neutrons. This is indeed the case for hydrogen and carbon, which have been calculated as 0.61 and 1.31×10^{-24} cm^2, respectively, for 15-Mev neutrons by Salant and Ramsay,[20] and as 2.40 and 1.96×10^{-24} cm^2 for 2.88-Mev neutrons by Zinn, Seely, and Cohen.[21] The values stated above for N, O, and S are higher than those obtained by the latter group, namely, 1.38, 1.25, and 3.12×10^{-24} cm^2.

[19] J. R. Dunning, Phys. Rev. **45**, 586 (1934).
[20] E. O. Salant and N. Ramsay, Phys. Rev. **57**, 1985 (1940).

Transition Gas Pressures

The dimensions of the large ionization chambers were chosen so that in at least one the transition pressure, $p_{G(j)}$, of the type j nuclei of the gas G, lies within the pressure range available for use. For the short range C, O, N, and A recoils in CO_2, O_2, N_2, and A the 3.3-cm diameter brass chamber was most useful, yielding the curves in Fig. 5, which clearly indicate the $p_{G(j)}$ regions. Since these pressures vary with the ranges of the particles, many of which are less than the maximum, the pressures stated in Table VII are approximate values. The table also includes the pressures measured with the 7.6-cm brass chamber or with the 10-cm gas-walled chamber for alpha-particles in He, Fig. 2, and for protons in CH_4 and C_2H_4, Fig. 3, and the resulting calculated transition pressures for small chambers with dimensions those of the thimble and cylindrical chambers. With He, CH_4, and C_2H_4 in the small chambers these pressures are greater than those employed; hence the parabolic shape of the gas ionization curve impresses a continuous curvature on the resultant experimental curve (Figs. 6b and 7b). The argon recoils have such short ranges that even with the smallest chamber ionization-

[21] W. H. Zinn, S. Seely, and W. V. Cohen, Phys. Rev. **56**, 260 (1939).

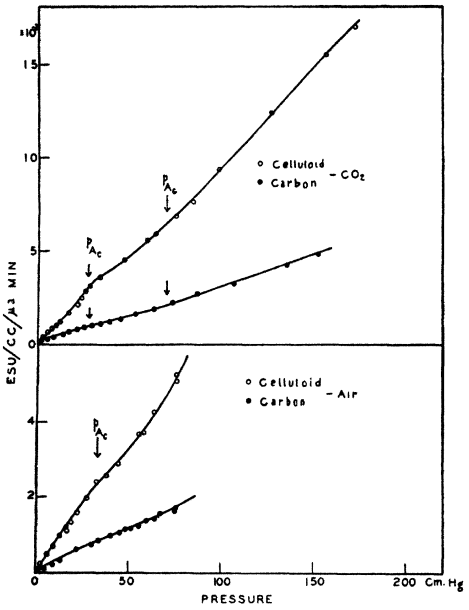

FIG. 6a. Cylindrical chamber curves showing transition pressures for wall and gas nuclei in air and in carbon dioxide.

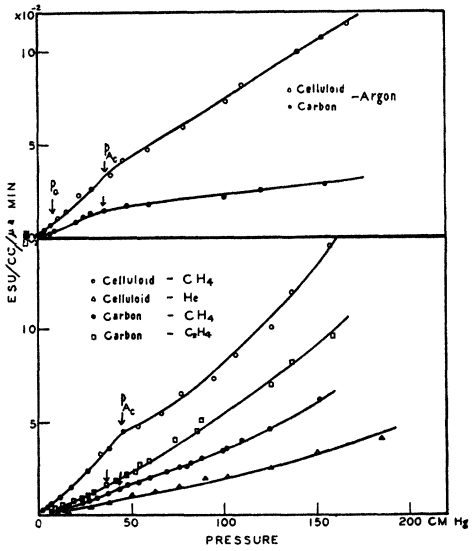

FIG. 6b. Cylindrical chamber responses in argon and in methane, ethylene, and helium.

pressure curves are practically linear throughout. With air and CO_2 the onset of linearity at the predicted pressures is easily identified in the thimble chamber curves (Fig. 7); with CO_2 and A it is observable in the cylindrical chamber results (Fig. 6).

Ranges and Energies of Recoiling Nuclei

From the transition pressures, the limiting dimensions of the containers, and the stopping powers of the gas for heavy particles, the maximum ranges of the various recoiling nuclei in their respective gases and the corresponding ranges in air have been calculated (Table VII). From the range-energy curves of Blackett and Lees[22] and Feather[23] for N, O, and C nuclei recoiling in alpha-particle collisions, the energies of these particles have been estimated. The range found for the A nuclei is considerably less than any studied by Blackett and Lees, hardly justifying an extrapolation for range. Since in elastic collisions (Eq. (2)), the maximum energy of C, N, O, and A recoiling nuclei is 0.28, 0.25, 0.22, and 0.10, respectively, of the incident neutron energy, a large portion of the neutrons entering the chambers must have energies of at least 5 Mev, the value mentioned earlier in this paper as calculated from the proton and alpha-particle ranges in hydrogenous gases and in helium, respectively.

Wall Effects in Small Chambers

For the wall effect analysis, thimble chambers with carbon, Bakelite, amber, brass, tin, or lead walls and cylindrical chambers with carbon or celluloid walls were irradiated. Short range heavy

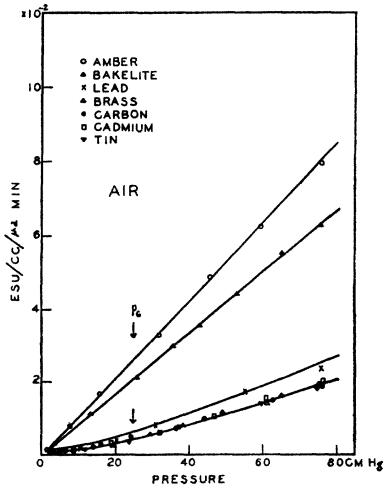

FIG. 7a. Thimble chamber responses in air.

[22] P. M. S. Blackett and D. S. Lees, Proc. Roy. Soc. **A134**, 658 (1931); **A136**, 325, 338 (1932).
[23] N. Feather, Proc. Roy. Soc. **A141**, 194 (1933).

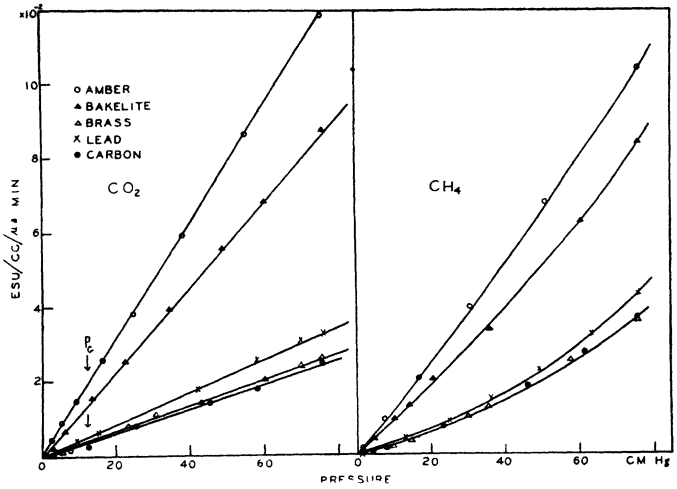

FIG. 7b. Thimble chamber responses in carbon dioxide and in methane.

nuclei are present in all these materials; protons are also present in amber, Bakelite, and celluloid walls. The ionizing effects of the C, N, and O wall particles are not easily separable from the effects of the gas nuclei, when measurements are made in gases containing these nuclei, but are strikingly separable in argon, since the ranges of the latter are less than a tenth of the C, N, and O ranges. The $i-p$ curves obtained when this gas is used in cylindrical chambers, particularly in the carbon chamber, Fig. 6b, indicate that at pressures exceeding 10 cm (at which the gas effect becomes linear), the curves are practically linear to about 35 cm, the slope then decreasing to about 50 cm, becoming linear again at higher pressures. At 35-cm pressure the longest range carbon particles are just able to cross the 0.74-cm limiting dimension obliquely to the tangent plane just across the chamber. At still higher pressures the energy of all is completely utilized in the chamber, producing $Q_{A(c)}/W_G$ ions.

The results obtained when these cylindrical chambers were filled with air, CO_2, or C_2H_4 (Fig. 6) also indicate the pressures $p_{A(c)}$, since the directions of the C, O, and N gas particles are much more at random than those emitted by the walls, so that the gas components of the $i-p$ curves remain parabolic to higher pressures determined by the 0.2-mm distance between the chamber walls. The resulting values of the ranges of the C and O wall nuclei agree, with these reservations, very well with those obtained directly from the "gas effect."

In thimble chambers transition pressures for heavy wall particles in the gases studied, air, CO_2, CH_4, and A are, with the exception of CH_4, about the same as those for the gas recoils; hence ionizing energy lost in the walls by gas recoils is very nearly compensated by that gained from recoiling wall particles. Ionization curves are linear except at the lowest pressures, the error introduced by assuming complete compensation being not more than 3 percent. Hence in the case of many non-hydrogenous-walled chambers the analysis $I_{A(c),G}+\sum I_{G,G}(k)$ may be replaced by the expression $I_{G,G}=Q_G/W_G$, where $Q_G=\sum_k Q_k$. That is, $I_{G,G}$ is the ionization which occurs in the gas when there is secondary particle equilibrium, its magnitude being proportional to the gas pressure, as are the other two components of the ionization caused by wall protons and by gamma-rays.

Consequently the fast neutron responses of thimble chambers with non-hydrogenous walls are practically the same (Fig. 7), the excess ionization in chambers with heavy walls such as lead being attributable to additional gamma-ray absorption. The relative gamma-ray responses of these chambers at atmospheric pressure have already been reported by Aebersold. They are shown at various pressures in Fig. 8. The ionization is linear with pressure, approximately four

times as dense as in 100-cc chambers (Fig. 4), the same in carbon, Bakelite, amber, brass, and cadmium-walled chambers, and is approximately 40 or 70 percent higher in chambers with tin or lead walls. The greater intensity undoubtedly results from the large ratio of the surface area to the volume of these small chambers. Similar relative gamma-ray effects must occur in neutron bombardment. Recalling that the ionizing electrons are not able through magnetic deflection to escape from the chambers before complete transit, it is reasonable to assume that in air in a carbon chamber the gamma-ray component is approximately 20 percent of the total response, and to calculate the component in the other chambers from the relative gamma-ray sensitivities revealed in Fig. 8. Since the stopping power of CO_2 is 50 percent higher than that of air, gamma-ray components in this gas must be correspondingly greater (Table VIII). The validity of an assumption of such high percentage of gamma-ray effects is shown both by the similar values calculated for $I_{G,G}$ in the various chambers for the two gases and by their relative values, shown in the same table, the CO_2/air ratio being 1.10, a quantity agreeably close to that obtained from alpha-particle measurements of the absorption of energy by the gas, namely, 1.113. Since under corresponding conditions the magnitudes of the gamma-ray responses of amber, Bakelite, and carbon must be practically the same (Fig. 8), only 5–6 percent of the total ionization measured in the amber and Bakelite chambers can be attributed to gamma-ray effects.

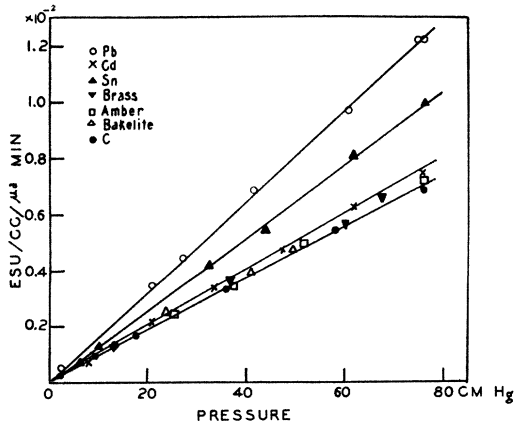

FIG. 8. Gamma-ray responses of air-filled thimble chambers. Ionization densities are nearly four times the densities obtained with 100-cc chamber (Fig. 4).

The excess response of chambers with hydrogenous walls over that of carbon-walled chambers must result from protons in the walls, the ratio of this proton component to the gas component being determined by

$$\frac{I_{A(p),G}}{I_{G,G}}=\frac{Q_{A_p}N_{T,p}S_{G(p)}}{Q_GN_AS_{A(p)}}=\frac{E_{A(p)}S_{G(p)}}{E_GS_{A(p)}},$$

where the E's represent the energies absorbed per molecule of the respective media. To test this relation, values of the energy absorbed by the protons per molecule were calculated from the values of E_m listed in Table IX and from the stopping powers per molecule relative to air calculated from the stopping powers of the atomic constituents, those of H and C being the values given by Livingston and Bethe for 3.26-Mev protons and that of O, the alpha-particle value. The molecular formulae and physical constants employed in this and further calculations are listed in Table X. The values of the ratios of the proton and gas recoil components of the ionization in amber and Bakelite chambers in air and CO_2 thus obtained are in excellent agreement, considering the possible contributing errors, those of the estimation of the gamma-ray component and of the uncertainties in the molecular formulae of the materials and in their stopping powers for high energy protons and heavy particles.

Finally, the energy absorbed by protons per cc of these wall materials, the quantity needed for the interpretation of biological experiments, has been calculated in three ways, directly through Eq. (11) from the proton component of the ionization (Table VII), indirectly from the product of the ratio of the proton and gas recoil components of the ionization (same table) and the energy E_G absorbed per gas molecule calculated from the values of E_j measured in the gas effect (Table VI) through the equation

$$Q_{A(p)}=E_G\frac{I_{A(p),G}}{I_{G,G}}N_A\frac{S_{A(p)}}{S_{G(p)}},$$

and directly from the product of the energy $E_{A(p)}$ absorbed by the protons per molecule calculated from the E_j's, and the number of mole-

TABLE VIII. The components of the ionization in thimble chambers (ionization expressed in e.s.u./cc/μamp. min. per cm pressure $\times 10^{-4}$).

Chamber wall	Total ionization in air	Total ionization in CO_2	Gamma-ray percentage air	Gamma-ray percentage CO_2	Neutron effects: Gas-wall component air	Gas-wall component CO_2	Proton component air	Proton component CO_2	Proton/gas ratio air exp.	Proton/gas ratio air calc.	Proton/gas ratio CO_2 exp.	Proton/gas ratio CO_2 calc.
Carbon	2.64	3.40	20	30	2.12	2.38						
Brass	2.88	3.60	22	33	2.15	2.40						
Cadmium	2.76		22	33	2.11							
Lead	3.26	4.64	34	51	2.15	2.28						
Amber	10.80	16.04	5	8	10.28	15.02	8.16	12.64	3.85	3.95	5.32	5.39
Bakelite	8.24	11.72	6	9	7.72	10.70	5.60	8.32	2.66	2.63	3.50	3.61

cules, N_A per cc. The excellent agreement in the results so obtained (Table IX) indicates that any one of the three methods may be used for calculation of the energy absorbed by the protons of hydrogenous material.

NEUTRON EFFECTS IN TISSUE

Energy Calculations

The last described method has been used to calculate the energy absorbed per g of various "tissues" and tissue-like materials frequently used for the walls of small ionization chambers. A molecular formula for tissue, stated in Table X, has been derived on the assumption that tissue is 85 percent water and 15 percent protein, the formula for protein being the average of those indicated from the analyses[24] of several tissue proteins. The energies absorbed per gram in such substances and in the tissue represented by the formulae proposed by Gray and Read[3] and by Zimmer[25] are given in the table, together with values for several gases, whose suitability for use in such chambers is discussed in this paper.

The calculations indicate that the response of amber to fast neutrons is very nearly that of tissue A, surpassing the responses of Bakelite and Aerion, materials most frequently used for the walls of the small chambers employed in dosimetry. The response of celluloid is similar to that of the protein molecule. It is obvious that if Aerion is used as a chamber wall, the ionization response will be much less than for a tissue wall and a large correction factor will be necessary in calculating the energy absorption in tissue.

Amber and Bakelite are not electrically conducting whereas Aerion is; consequently the conducting layer with which amber and Bakelite chambers must be lined causes some loss of energy of the protons emerging from the hydrogenous walls and the layer itself will contribute no protons. The graphite conducting layers used in these chambers have been varied from thicknesses quite translucent to light to those opaque with a resultant variation of the ionization response of only a few percent. Very thin layers were sufficient to form the conducting layer. The average path length of a proton in crossing the chambers must have been of the order of 0.5 cm, the range of a recoil proton of energy 0.3 Mev. To penetrate a carbon lining opaque to light and to cross the chamber the proton must have 0.4 Mev of energy, a negligible fraction of the predominant energy (5 Mev) indicated by transition pressures.

The advantage of the hydrocarbons as wall materials results both from the relative fractions of the energy absorbed by the nuclei involved and from the relative collision cross sections. Since the latter are energy dependent, varying widely between the 2- and 16-Mev regions commonly studied, it follows that the relative energies absorbed per gram by tissue-like substances

TABLE IX. Energy in ergs absorbed by protons per cc of hydrogenous material per μamp. min. of deuteron charge at 85 cm from target.

Material	Source of calculation: Proton component in "wall effect" air	Proton component in "wall effect" CO_2	Proton/gas ratio air	Proton/gas ratio CO_2	"Gas effect" (Table X)
Amber	6.80	6.82	6.86	6.87	6.64
Bakelite	4.16	4.03	4.26	4.18	4.00

[24] H. S. Sherman, *Chemistry of Food and Nutrition* (The Macmillan Company, New York, 1937), fifth edition, pp. 57–66.

[25] N. W. Timozeeff-Ressovsky and K. G. Zimmer, Naturwiss. **26**, 362 (1938).

TABLE X. Neutron energy absorbed per μamp. min. of 8-Mev deuterons on Be.

Material	Formula[a]	M	Number of molecular groups per cc[b]	Stopping power per molecular group	Energy absorbed in "e" units[c]	Percent absorbed by protons
Amber	$C_5H_8O_{0.5}$	76.0	8.24×10^{21}	3.35	7.35	88
Bakelite	$C_7H_8O_2$	124.0	6.44	5.05	4.98	80
Celluloid	$C_{5.3}H_8O_{3.5}N_{0.7}$	129.2	6.35	5.29	4.53	80
Aerion	$C_{10.9}H_8O_{2.7}$	100.4	4.81	7.46	3.73	77
Tissue[d] *A*	$C_{0.5}H_8O_{3.8}N_{0.14}$	75.0	7.80	3.13	7.11	90
Tissue *B*	$C_{0.8}H_8O_4$	71.6	7.40	3.67	6.68	88
Tissue *C*	$C_{5.2}H_8$	70.4	8.60	3.18	7.96	87
Water	$4(H_2O)$	72	8.42	3.16	7.40	88
Paraffin	$4(CH_2)$	56	9.72	2.64	9.55	89
Air	$O_{0.4}N_{1.6}$	28.8	0.027	1.00	1.38	0
Oxygen	O_2	32	0.027	0.99	0.84	0
Carbon dioxide	CO_2	44	0.027	1.50	0.96	0
Ethylene	$2(C_2H_4)$	56	0.013	2.64	9.55	89

[a] Formulae for hydrogenous materials adjusted to give equivalent proton constituents.
[b] Calculated from density and molecular formula. Density of tissue taken as unity.
[c] Authors propose use of unit "e," 1 erg of energy absorbed per g of material.
[d] Tissue *A* taken as 15 percent protein and 85 percent water. Approximate protein formula was calculated from analyses of beef muscle tissue, egg albumin, casein, and gelatin, quoted by Shermann (see reference 24). Tissue *B* is formula given by Gray and Read (see reference 3). Tissue *C* is formula given by Zimmer (see reference 25).

must vary, as is indicated in Table XI by the ratios of the energy absorbed by tissue molecules and by air and oxygen, calculated from selected values of cross sections appearing in the literature. The observations of Salent and Ramsay[22] are for H and C alone, the proton value being a fraction of that quoted by Kichuchi and Aoki[26] for the same energy range; hence, if the former values are combined with the O and N values of the latter, much lower absorbed energies are indicated. According to the calculations the protons from less energetic neutrons, 2–3 Mev, are relatively more effective than those from higher energy neutrons. Neutrons with the lower energies as well as soft neutrons must be abundant in the beams used in neutron therapy, particularly after penetration of the skin and tissue to the depth of the section under treatment. Lacking direct knowledge of the energy distribution of the beam, measurements such as those herein described should be conducted for the various operating conditions.

Calculation of Energy Absorbed in Tissue from Ionization Measurements

For the dosimetry measurements incidental to the interpretation of the effects of neutron irradiation of biological specimens the energy absorbed from the beam must be calculated directly from simultaneous ionization measurements utilizing either "gas-effect" large chambers or "wall-effect" small chambers. In the former case the energy is calculated by first correcting the gas ionization for its gamma-ray component and then calculating the neutron energy absorbed per gram of the gas and multiplying this by the tissue/gas ratio given in Table XI. It is often suggested that the gas employed might well have atomic constituents equivalent to those of the tissue, such as C_2H_4 or some composition gas. But the recoil protons of such gases have long ranges, the limiting pressures at which secondary particle equilibrium sets in is several atmospheres, and because of the parabolic $i-p$ relationship below this pressure the assumption of proportionality between responses and densities of the gas is erroneous. For example, with C_2H_4 at atmospheric pressure in the large wire chamber used in the experiments reported in this paper the response is 51 percent of that calculated from $p(W_G dI_G/dp)$; in a chamber of about 1-cm dimensions the response would be less than 10 percent of the theoretical value. In non-hydrogenous gases, on the other hand, the range of the recoil nuclei is short and the gas response is very nearly proportional to its density. Although air is commonly used, oxygen is a more suitable gas, since in nitrogen-containing gases a considerable proportion of the ionizing particles released by neutron irradiation are nuclear

[26] S. Kichuchi and A. Aoki, Proc. Phys. Math. Soc. Japan 21, 75 (1939).

TABLE XI. Energies absorbed per g of tissue-like substances relative to air and O_2, calculated from cross sections obtained at various neutron energies.

Neutron source and energy	Observers	Ratios of energies absorbed calculated for relative to	amber	Bakelite	tissue A[a]
D—Be 5 Mev	Aebersold and Anslow	air	5.3	3.6	5.2
		O_2	8.8	5.9	8.4
D—D	Zinn, Seely, and Cohen (see reference 21)	air	12.7	8.0	12.3
		O_2	16.5	10.9	16.0
D—D	Kichuchi and Aoki (see reference 26)	air	10.4	6.8	10.2
		O_2	13.9	9.0	13.4
D—Li	Kichuchi and Aoki (see reference 26)	air	6.3	4.2	6.2
		O_2	10.8	7.2	10.6
D—Li[b]	Salant and Ramsay (see reference 20) with Kichuchi and Aoki	air	3.0	2.2	3.1
		O_2	5.2	3.6	5.3

[a] See note with Table VI.
[b] The H and C cross sections of Salant and Ramsay are combined with the N and O cross sections of Kichuchi and Aoki.

disintegration products, whereas in both oxygen and tissue practically all are recoil nuclei.

When small chambers are utilized for the calculation, the energy may be estimated quite simply from the response of a chamber with hydrogenous walls, such as a Victoreen thimble chamber with Bakelite walls, through an extension of the Bragg-Gray law to relate the energies absorbed by tissue and by chamber walls to the ionizations produced in the two media.

Since a high percentage of the ionization effected in tissue is produced by recoil protons the energies absorbed by the protons in the respective walls may be used for the calculations. The proportionality existing between these energies and the respective proton densities is expressed by

$$Q_{T(p)}/Q_{A(p)} = p_T N_T / p_A N_A, \tag{16}$$

where subscripts T refer to tissue and A to chamber walls, and p represents the number of protons per molecule, N being the number of molecules per cc.

The Bragg-Gray relationship states that for tissue

$$Q_{T(p)\text{per cc}} = W_{T(p)} I_{T(p),\, T\text{per cc}}, \tag{17}$$

and that for the chamber walls

$$Q_{A(p)\text{per cc}} = W_{G(p)} \frac{N_A s_A}{N_G s_G} I_{A(p),\, G\text{per cc}}. \tag{11}$$

Combining Eqs. (11) and (16) and reducing unit volume to unit mass measurements, we obtain

$$Q_{T(p)\text{per gram}} = k_n W_{G(p)} I_{A(p),\, G\text{per gram}} = k_n E_{A(p),\, G\text{per gram}}. \tag{18}$$

Here $E_{A(p),G\text{per gram}}$ is the energy transferred to a gram of the gas by the ionizing protons released from a gram of the wall material and

$$k_n = p_T M_G s_A / p_A M_T s_G, \tag{19}$$

i.e., the product of the ratio of the proton contents of the tissue and the wall molecules, the ratio of the molecular weights of the gas and the wall material, and the ratio of the molecular stopping powers of the wall material and the gas.

Stopping powers of the hydrogenous materials in question may be calculated by recourse to the stopping power curves given by Livingston and Bethe, which give the dependence of proton stopping powers on their energy. These stopping powers also depend on the atomic composition of the materials. Typical values for such stopping powers relative to air are listed in Table XII for amber, Bakelite, and Aerion chamber walls. Corresponding values of k_n are given in Table XIII. Since the proton energies involved do not exceed 4 Mev, it appears that values of k_n applicable to the reduction of chamber readings such as those given in Table VIII to tissue effects are approximately 4/3, 2, and 3 for amber, Bakelite, and Aerion, respectively.

If studies are being made of physiological effects at considerable depths within the tissue, consideration must be given to the softening effect of successive neutron collisions and the

TABLE XII. Dependence on proton energy of stopping-powers of hydrogenous walls.

Wall material \ Proton velocities in 10^9 cm/sec. / Proton energies in Mev	1.0	1.5	2.0	2.5	3.0	4.0
	0.52	1.17	2.09	3.26	4.70	8.36
Amber	3.67	3.50	3.41	3.35	3.32	3.26
Bakelite	5.41	5.22	5.12	5.05	5.00	4.95
Aerion	7.71	7.68	7.55	7.44	7.37	7.30

TABLE XIII. Dependence of k_n for monochromatic neutrons on proton energy and chamber walls.

Wall material \ Proton energies in Mev	0.52	1.17	2.09	3.26	4.70	8.36
Amber	1.48	1.40	1.36	1.34	1.33	1.31
Bakelite	2.16	2.09	2.04	2.01	2.00	1.98
Aerion	3.13	3.03	3.00	2.95	2.92	2.90

consequent increase of neutron cross sections. In such cases larger values of k_n than those listed in Table XIII must be selected. By choosing a value of 2.5 for the reduction factor, which reduces Victoreen Bakelite chamber readings (called n units when used for measuring fast neutrons) to tissue dosage, the staff of the Crocker Laboratory at Berkeley has recognized the effect of such soft neutrons within the tissue, and also the ionization which results from the heavier nucleus recoils and the accompanying gamma-rays.

It is believed that biological effects result from the action of the highly energized ions produced from the water of tissue on the protein molecules. Therefore, $I_{T(p),T}$ rather than $Q_{T(p)}$ should be calculated. This can be done through Eqs. (17) and (18). The evaluation can be completed only if W_G/W_T is known. Although the values of the W's must vary with proton energies, relative values must be nearly constant. Moreover W_G/W_T must approximate W_G/W_{H_2O}. Although W_{H_2O} has not been measured, it may be assumed to be about 26 ev, twice the ionizing energy for H_2O. It is not proper to estimate W_{tissue}, as frequently suggested, from the average energy required to produce ion pairs in a gas mixture with atomic constituents those of tissue, since the ionization potentials of large hydrocarbons are larger than those of the smaller molecules of the mixture.

Relative Effectiveness of Neutron and X-Irradiation of Tissue

In many biological studies it is not necessary to evaluate W_T, for frequently the relative ionizations produced in the medium by the two types of radiation are adequate. Ionization effects produced by x-rays are caused by recoiling electrons, the energy absorbed being proportional to the number of electrons per unit mass or volume of the substance and to the conversion coefficient of photon energy to kinetic energy of electrons. This coefficient is the sum of the respective coefficients for photoelectrons, Compton recoils, and electron pairs. Using primed letters to represent x-ray effects we have

$$I'_{T(e)}=I'_{A(e),G}\frac{Q'_{T(e)}W'_{G(e)}S'_A}{Q'_{A(e)}W'_{T(e)}S_G'}$$

or

$$I'_{T(e)}=I'_{A(e),G}\frac{Z_TN_Tk_{e,T}W'_{G(e)}}{Z_GN_Gk_{e,A}W'_{T(e)}} \tag{20}$$

since

$$\frac{Q'_{T(e)}}{Q'_{A(e)}}=\frac{Z_TN_T}{Z_AN_A}\frac{k_{e,T}}{k_{e,A}};\quad\text{and}\quad\frac{S_A'}{S_G}=\frac{Z_AN_A}{Z_GN_G}.$$

where Z is the number of electrons per molecule, N is the number of molecules per gram, and k_e is the fraction of photon energy converted per electron to kinetic energy of secondary electrons. Consequently, the energy absorbed per gram of tissue is

$$Q'_{T(e)\text{per gram}}=W'_{T(e)}I'_{T(e),T\text{per gram}}$$

$$=k_xW'_{G(e)}I'_{A(e),G\text{per gram}} \tag{21}$$

where

$$k_x=\frac{Z_TM_Gk_{e,T}}{Z_GM_Tk_{e,A}}. \tag{22}$$

Values of the conversion coefficients (k_e) at various x-ray energies have been calculated by Mayneord[27] for tissue, air, nitrogen, and oxygen. These are nearly the same for the gases and practically the same for tissue. Even for soft radiations the tissue value is hardly 10 percent less than that for air. Hence the energy absorption per gram in tissue must be nearly that in these gases and the value of k_x is very close to unity.

Finally, the ratios of the energies absorbed and of the resulting ionizations produced by x-rays

[27] W. V. Mayneord, Brit. J. Radiol. 8, 235 (1940).

and neutron beams is given by

$$\frac{Q'_{T(e)}}{Q_{T(p)}}=\frac{I'_{T(e),T}}{I_{T(p),T}}=\frac{k_x}{k_n}\frac{I'_{A(e),G}}{I_{A(p),G}}=K\cdot r/n \quad (23)$$

where $K=k_x/k_n$, and r and n are the exposures of the x-ray and neutron beams measured in roentgens and n units, respectively. This equation holds for measurements made per unit volume or per unit gram of the materials. Since k_x is approximately unity, K is the inverse of k_n, whose value was discussed in the preceding section.

If, after the relative ionizing energies of x-ray and neutron beams have been so determined, disproportionate biological actions occur, they must result from the strikingly opposite character of the ionic distribution resulting from the two agents, i.e., the widely spread and relatively weak ionization along the paths of the electrons scattered by x-rays, and the concentrated and dense ionizations along the paths of nuclei recoiling from neutrons. As reported by Aebersold and Lawrence, inequalities in biological sensitivities have been observed in most investigations, the relative sensitivities apparently resulting from the physiological condition of the irradiated material.

The authors gratefully express their appreciation of the interest and valuable assistance given them by members of the Radiation Laboratory, particularly Dr. K. McKenzie, and thank Professor E. O. Lawrence and the staff of the Laboratory for their cooperation in making available long periods of cyclotron time. The work was made possible by the generous support of the Rockefeller Foundation and the Josiah Macy, Jr. Foundation. One author was enabled to participate in the research through a fellowship awarded by the Finney-Howell Foundation, the other through a grant from the Trustees of Smith College.

PHYSICAL REVIEW VOLUME 69, NUMBERS 1 AND 2 JANUARY 1 AND 15, 1946

Activity of N^{16} and He^{6}

H. S. SOMMERS, JR.* AND R. SHERR*
Jefferson Physical Laboratory, Harvard University, Cambridge, Massachusetts
(Received August 28, 1945)

An interrupted flow method of handling short lived gases is described. By use of the method, pure N^{16} and pure He^{6} are readily produced. Geiger counter measurements on the N^{16} give a period of 7.3 ± 0.3 sec. Presence of gamma-rays having energy greater than 5 Mev is demonstrated with a cloud chamber and absorption measurements. A lower limit to the end point of the N^{16} spectrum is derived from absorption curves, and an upper limit fixed by excitation measurements. By taking into account the barrier of N^{16} against emission of a proton, and excluding the electron self-energy, the maximum electron energy of the decay may be set at 10 ± 0.5 Mev. The electron absorption curves show the beta-spectrum to be complex with a softer component having an end point at approximately 4 Mev corresponding to decay to an excited state of O^{16} in the region of 6 Mev. The He^{6} period found is 0.85 ± 0.05 sec., and its end point 3.5 ± 0.6 Mev, in agreement with Bjerge and Bröstrum.

Part I. N^{16}

A. INTRODUCTION

N^{16} WAS reported in 1934 by Fermi[1] and his co-workers and also by Livingston, Henderson, and Lawrence.[2] Both groups found a negative electron emitter with lifetime of nine or ten seconds formed by the bombardment of fluorine with neutrons, and both assigned it to the reaction $F^{19}(n|\alpha)N^{16}$. In 1936 Fowler, Del-

* Now at the Radiation Laboratory, Massachusetts Institute Institute of Technology, Cambridge, Massachusetts. This work was completed in 1942.

[1] Fermi, Amaldi, d'Agnostino, Rasetti, and Segrè, Proc. Roy. Soc. **A146**, 483 (1934).

[2] Livingston, Henderson, and Lawrence, Phys. Rev. **46**, 325 (1934).